

# Morphological and DNA analyses reveal cryptic diversity in *Anentome wykoffi* (Brandt, 1974) (Gastropoda: Nassariidae), with descriptions of two new species from Thailand

Nithinan Chomchoei<sup>A,B,C</sup>, Thierry Backeljau<sup>D,E</sup>, Piyatida Pimvichai<sup>F</sup>, Ting Hui Ng<sup>G,H</sup>  and Nattawadee Nantarat<sup>B,C,I,\*</sup> 

For full list of author affiliations and declarations see end of paper

**\*Correspondence to:**

Nattawadee Nantarat  
 Department of Biology, Faculty of Science,  
 Chiang Mai University, Chiang Mai, 50200,  
 Thailand  
 Email: [n\\_nantarat@yahoo.com](mailto:n_nantarat@yahoo.com)

**Handling Editor:**

Gonzalo Giribet

**Received:** 1 May 2023

**Accepted:** 6 October 2023

**Published:** 2 November 2023

**Cite this:**

Chomchoei N *et al.* (2023)  
*Invertebrate Systematics*  
**37**(11), 755–771. doi:[10.1071/IS23019](https://doi.org/10.1071/IS23019)

© 2023 The Author(s) (or their employer(s)). Published by CSIRO Publishing.

This is an open access article distributed under the Creative Commons Attribution-NonCommercial-NoDerivatives 4.0 International License ([CC BY-NC-ND](https://creativecommons.org/licenses/by-nc-nd/4.0/))

OPEN ACCESS

## ABSTRACT

The assassin snail genus *Anentome* is widely distributed in South East Asia. In Thailand, the genus comprises at least six species, one of which is *Anentome wykoffi*, a species that may act as an intermediate host of parasitic trematodes. Recent fieldwork has shown that *A. wykoffi* is far more common and widespread in Thailand than has been assumed, yet the taxonomy remains poorly known. Therefore, this study explores morphological and DNA sequence (*COI* and *28S* rRNA) variation in *A. wykoffi* to verify and finetune the taxonomic interpretation of this species. To this end, 12 populations of *A. wykoffi* were sampled in Thailand. This survey allowed us to preliminarily distinguish three putatively cryptic morphotypes. Shell shape measurements and geometric morphometric analyses revealed significant differences between these morphotypes, whereas SEM observations of the shell sculpture and radula confirmed the consistent separation of the three morphotypes. Finally, a combined phylogenetic and species delimitation analysis of *COI* and *28S* rRNA sequence data showed that the three morphotypes represent three well-supported clades, one of which is sister group to *A. cambojiensis*. As such, the three morphotypes as defined by (1) the presence or absence of a carinated shoulder, (2) the number of spiral lines on the spira and (3) the pattern of the central cusps on the central radular tooth, are interpreted as three different species under the morphological and phylogenetic species concepts but also likely under the biological species concept, viz. *A. wykoffi* (*sensu stricto*), *A. longispira* sp. nov. and *A. khelangensis* sp. nov. The three cryptic species are (re)described and the implications of separation are briefly discussed.

**ZooBank:** [urn:lsid:zoobank.org:pub:B39722E6-C915-4FA4-B03B-C15836B0DCAE](https://www.zoobank.org/urn:lsid:zoobank.org:pub:B39722E6-C915-4FA4-B03B-C15836B0DCAE)

**Keywords:** biodiversity, Gastropoda, Mollusca, morphology, morphometrics, phylogeny, systematics, taxonomy.

## Introduction

The gastropod family Nassariidae includes 12 genera with ~1320 extant nominal species (Galindo *et al.* 2016). Most of these species live in marine habitats, except for the freshwater genera *Anentome* Cossmann, 1901 (10 species), *Clea* H. Adams & A. Adams, 1855 (five species) and *Oligohalinophila* Neiber & Glaubrecht, 2019 (one species) (Adams 1855; Cossmann 1901; Galindo *et al.* 2016; Strong *et al.* 2017; Neiber and Glaubrecht 2019).

Species of the genus *Anentome* are commonly found in the broad lower reaches of coastal rivers, lakes and ponds in South-East Asia, including Cambodia, Indonesia, Laos, Malaysia, Singapore, Thailand and Vietnam (Brandt 1974). Six *Anentome* species have been reported from Thailand, viz. *A. cambojiensis* (Reeve, 1891), *A. helena* (von dem Busch, 1847), *A. jullieni* (Deshayes, 1876), *A. scalarina* (Deshayes, 1876), *A. spinosa* (Temcharoen, 1971) and *A. wykoffi* (Brandt, 1974). In particular, *A. helena* is a non-selective predator and scavenger that is highly popular in the aquarium trade, known as

the ‘assassin snail’ and used to control pest snails. Moreover, *A. helena* and *A. wykoffi* are intermediate hosts of trematode parasites, including *Echinostoma* sp. that may cause human echinostomiasis (Krailas et al. 2012; Chantima et al. 2013, 2018; Yutemsuk et al. 2017; Chomchoei et al. 2018, 2022; Butboonchoo et al. 2020; Wiroonpan et al. 2021, 2022). The vector capacity and global export of *A. helena* by the aquarium trade make the clarification of the biology and taxonomy of the genus *Anentome* important. In this context, Strong et al. (2017) and Chomchoei et al. (2018) provided morphological and DNA evidence suggesting that the taxonomy of *A. helena* may be more complex than previously assumed due to the presence of cryptic diversity.

This study continues along these lines by focusing on *A. wykoffi*, an endemic species in Thailand that until recently, was reported from only two localities in the Middle Mekong basin, viz. the type localities from Bandan (Fig. 1: locality 9) and Ubol Rattana Dam (Fig. 1: locality 2) (Brandt 1974; Kittivorachate and Yangyuen 2004). However, new fieldwork (e.g. Chomchoei et al. 2022) shows that the species is far more common and widespread in Thailand than previously assumed. Considering previous experience with respect to morphological and DNA sequence variation in *A. helena* and given that *A. wykoffi* was described based solely on shell morphology, we report morphological and DNA sequence variation of *A. wykoffi* from different river basins and drainage systems in Thailand (Fig. 1). We therefore attempt to improve the taxonomic interpretation of this poorly known species and describe two new closely related cryptic species.

## Materials and methods

### Ethics

All animal experiments were undertaken according to guidelines approved by the Institute of Animals for Scientific Purpose Development (IAD), National Research Council of Thailand (permit number U1-07724-2561, issued to Nithinan Chomchoei). This study complied with all the relevant national regulations and institutional policies for the humane care and use of animals.

### Collection abbreviations

CMUZ, Museum of Zoology, Chiang Mai University, Chiang Mai, Thailand.

MNHN, Muséum national d’Histoire naturelle, Paris, France. SMF, Forschungsinstitut und Naturmuseum Senckenberg, Frankfurt am Main, Germany.

ZRC, Zoological Reference Collection, Lee Kong Chian Natural History Museum, National University of Singapore, Singapore.

## Sampling and specimen identification

*Anentome wykoffi* specimens were collected in various river basins and drainage systems in Thailand (Fig. 1 and Table 1) using the count-per-minute method (Olivier and Schneiderman 1956). Thailand comprises five main river basins, including the Salween, Chao Phraya, Gulf of Thailand coast, Peninsular Malaysia and Mekong basins (Food and Agriculture Organization of the United Nations 2021) (Fig. 1), with the latter being further subdivided into three fish migration zones (upper, middle and lower Mekong; Fig. 1) (Mekong River Commission 2010). Specimens were preserved at  $-20^{\circ}\text{C}$  until being used to study morphology and DNA.

Identification of the specimens was primarily based on a comparison with photographs of the type specimens (Holotype SMF 219824 and Paratype SMF 225241) and the original description (Brandt 1974). *Anentome wykoffi* was hitherto likely only illustrated by Brandt (1974). Yet the species can be distinguished from *A. helena* by the well-rounded whorls, narrower costulation, thinner texture, shorter siphonal canal and lower number of whorls (*A. wykoffi* = 5, *A. helena* = 8) (Brandt 1974). For *A. wykoffi*, characters such as carination of the shoulder of the whorls, number of spiral lines on the spira and pattern of the central cusps on the central tooth of the radula were used to distinguish putative morphotypes as follows:

- (a) Morphotype A: shoulder not carinated, 3–5 spiral lines on the spira and central cusps of the central radular tooth similar in size.
- (b) Morphotype B: shoulder carinated, 3–5 spiral lines on the spira and central cusps of the central radular tooth similar in size.
- (c) Morphotype C: shoulder not carinated, 2 spiral lines on the spira and central cusp of the central radular tooth shorter than the two adjacent cusps.

## Shell measurements and geometric morphometric analyses

Shell dimensions, including shell height (SH), shell width (SW), apertural height (AH), apertural width (AW), last whorl height (LWH), last whorl width (LWW) and siphonal canal width (SCW) (Fig. 2a) were measured in mm with a digital Vernier calliper (BEC, G14032021) following Lee et al. (2022). The shell height without the last whorl (SH-LWH) was calculated as shell height minus last whorl height and spira height (SPH) was calculated as shell height minus apertural height. The following ratios were calculated: SH/SW, AH/AW, SH/AH, SW/AW, SH/LWH, LWH/(SH-LWH), LWH/AH, SPH/AH, SW/LWW, LWW/AW, SW/SCW, AW/SCW, LWW/SCW, LWH/SH, AH/SH and SPH/SH. A one-way analysis of variance (ANOVA) was applied with IBM SPSS Statistics software (ver. 20, IBM Corp.) to analyse the variation in shell parameters between putative morphotypes.

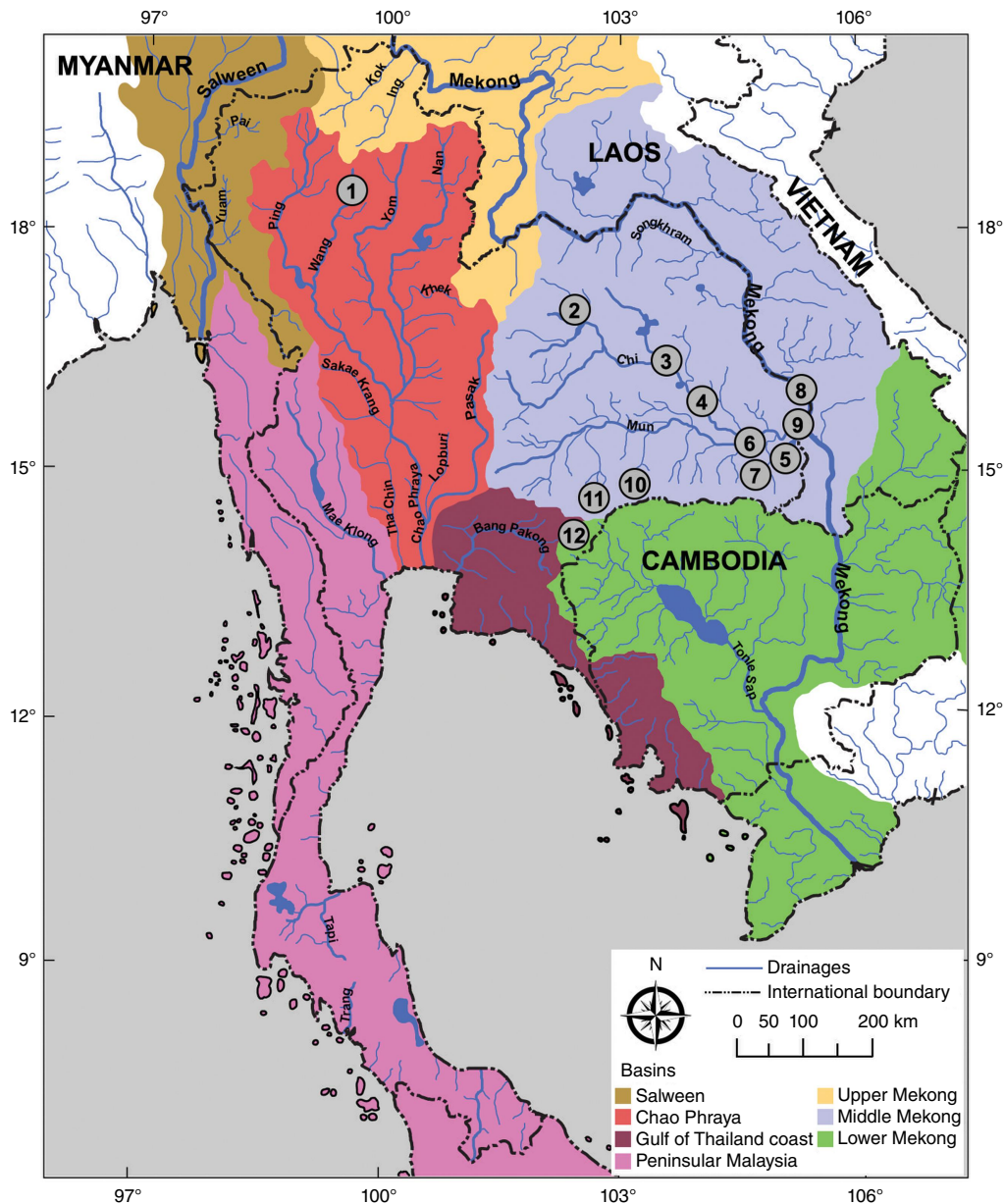


**Fig. 1.** Sampling localities of *A. wykoffi* in the river basins of Thailand. The collecting site numbers refer to Table 1. The delimitation of the river basins is based on Mekong River Commission (2010) and Food and Agriculture Organization of the United Nations (2021).

Shells were photographed with a Nikon D5500 digital camera for the geometric morphometric study. The photos were randomly ordered in tpsUtil (ver. 1.82, see <https://tpsutil.software.informer.com/>; Rohlf 2015). Fifteen landmarks on the shells were digitised on photos by the same person using the program tpsDig2 (ver. 2.29, see <https://tpsdig2.software.informer.com/>; Rohlf 2015) (Fig. 2b). Geometric morphometric analyses were performed with the software package MORPHOJ (ver. 1.06d, see [https://morphometrics.uk/MorphoJ\\_guide/frameset.htm?changelog.htm](https://morphometrics.uk/MorphoJ_guide/frameset.htm?changelog.htm); Klingenberg 2011). Canonical variance analysis (CVA) based on shell shape variation between putative

morphotypes was examined. Pairwise Mahalanobis distances and Procrustes distances between putative morphotypes were assessed for significant differences by a permutation test (10 000 iterations). Photos of the type specimens from this study were deposited in Morphobank (<http://morphobank.org/permalink/?P4892>).

### Scanning electron microscopic (SEM) study of the shell and radula

Shells were washed with distilled water several times and air dried to study shell microsculpture (Coppo and De Vos

**Table 1.** List of collecting sites of *Anentome* species and outgroup samples, and Genbank accession numbers of *COI* and *28S* rRNA sequences used in this study.

Map number	Species or voucher ID	Locality	GPS coordinates	Drainage (basin)	Genbank accession numbers	
					<i>COI</i>	<i>28S</i> rRNA
<i>Anentome wykoffi</i>						
1	CMUZ A193001	Huai Mae Nueang, Mueang Pan, Lampang, Thailand	18°32'04.0"N, 99°28'26.8"E	Wang (Chao Phraya)	OP955862	OP955888
	CMUZ A193002				OP955863	OP955889
2	CMUZ A213003	Ubol Ratana Dam, Nong Ruea, Khon Kaen, Thailand	16°32'10.7"N, 102°31'01.4"E	Chi (Middle Mekong)	OP955864	OP955890
3	CMUZ A193004	Huai Kut Daeng Reservoir, Chaturaphak Phiman, Roi Ed, Thailand	15°50'55.0"N, 103°33'44.7"E	Chi (Middle Mekong)	OP955865	OP955891
	CMUZ A193005				OP955866	OP955892
4	CMUZ A193006	Phaya Thaen Public Park, Mueang, Yasothorn, Thailand	15°47'23.0"N, 104°09'13.0"E	Chi (Middle Mekong)	OP955867	OP955893
	CMUZ A193007				OP955868	OP955894
5	CMUZ A213008	Mun River Bridge, Khong Chiam, Ubon Ratchathani, Thailand	15°18'30.2"N, 105°29'36.4"E	Mun (Middle Mekong)	OP955869	OP955895
	CMUZ A213009				OP955870	OP955896
6	CMUZ A193010	Sirindhorn Dam, Sirindhorn, Ubon Ratchathani, Thailand	15°12'37.8"N, 105°25'36.0"E	Mun (Middle Mekong)	OP955871	OP955897
	CMUZ A193011				OP955872	OP955898
7	CMUZ A213012	Lam Dom Noi, Buntharik, Ubon Ratchathani, Thailand	14°38'33.0"N, 105°22'06.8"E	Mun (Middle Mekong)	OP955873	OP955899
8	CMUZ A213013	Mekong River, Khemmarat, Ubon Ratchathani, Thailand	16°02'37.4"N, 105°13'27.0"E	Mekong (Middle Mekong)	OP955874	OP955900
9	CMUZ A213014	Mekong River, Ban Dan, Khong Chiam, Ubon Ratchathani, Thailand	15°19'05.5"N, 105°30'09.4"E	Mekong (Middle Mekong)	OP955875	OP955901
	CMUZ A213015				OP955876	OP955902
	CMUZ A213016				OP955877	OP955903
10	CMUZ A213017	Huai Dan Reservoir, Kap Choeng, Surin, Thailand	14°26'18.5"N, 103°42'35.1"E	Mun (Middle Mekong)	OP955878	OP955904
11	CMUZ A213018	Lam Nang Rong Dam, Non Din Daeng, Buri Ram, Thailand	14°17'42.7"N, 102°45'31.6"E	Mun (Middle Mekong)	OP955879	OP955905

(Continued on next page)

Table 1. (Continued)

Map number	Species or voucher ID	Locality	GPS coordinates	Drainage (basin)	Genbank accession numbers	
					COI	28S rRNA
12	CMUZ A213019	Hui Phrom Hot, Aranyaprathet, Sa Kaeo, Thailand	13°40'05.6"N, 102°31'24.8"E	Tonle Sap (Lower Mekong)	OP955880	OP955906
	CMUZ A213020				OP955881	OP955907
	CMUZ A213021				OP955882	OP955908
	MNHN IM 2013-52176	Sam Phan Bok, Pho Sai District, Ubon Ratchathani, NE Thailand, Mekong River, Thailand	–	Mekong (Middle Mekong)	KY773628	KY706439
<i>Anentomeambojiensis</i>	ZRC.MOL.015712	Tonle Sap Lake open area near Chong Khneas, Chong Khneas, Siem Reap Province, Cambodia	12°30'20.1"N, 103°50'06.2"E	Tonle Sap (Lower Mekong)	OQ832701	–
	CMUZ A213022	Tonle Sap River in Kaoh Thkov, Chol Kiri, Kampong Chhnang Province, Cambodia	12°03'31.7"N, 104°46'22.4"E	Tonle Sap (Lower Mekong)	OP955883	OP955909
<i>Anentome costulata</i>	CMUZ A193023	Urai Thong Cave, Kamphaeng, La-ngu, Satun, Thailand	6°56'15.7"N, 99°45'52.1"E	Rangu (Peninsular Malaysia)	OP955884	OP955910
	CMUZ A193024				OP955885	OP955911
<i>Anentome helena</i>	MNHN IM 2013-52184	FW Pond in Phuket Park Thailand	–	(Peninsular Malaysia)	KY773634	KY706444
	MNHN IM 2013-52185				KY773635	KY706445
<i>Oligohalinophila dorri</i>	MNHN IM 2009-20638	Song Luy River, Phan Ri Cua, Binh Thuan Province, Vietnam	11°10.57'N, 108°33.70'E	Song Luy	KY773620	KY706430
	MNHN IM 2009-20640				KY773621	KY706431
	MNHN IM2009-20644				KY773624	KY706434
<i>Nassarius arcularia</i>	MNHN IM 2007-31898	Panglao Island, inside lagoon near Doljo Pt, Philippines	9°35.1'N, 123°43.6'E	–	KY451259	KY489161
<i>Nassarius boucheti</i>	MNHN IM 2009-21554	Ounia Pass, New Caledonia	21°52'S, 166°51'E	–	KY451266	KY489176

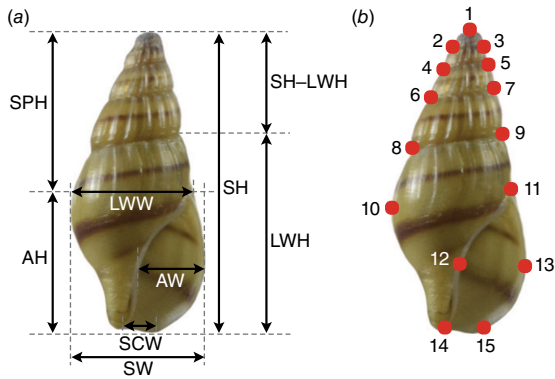


**Fig. 2.** Shell measurements (a) and landmarks (b) of *A. wykoffi* used in this study. Shell height (SH), shell width (SW), apertural height (AH), apertural width (AW), last whorl height (LWH), last whorl width (LWW), siphonal canal width (SCW), spira height (SPH) and shell height without the last whorl (SH-LWH)

1986). The shells subsequently were mounted on aluminium stubs using carbon conductive adhesive tape. The mounted shells were coated with gold and studied with an LV-Scanning Electron Microscope (JSM 5910 LV) at the Electron Microscope Research and Service Center, Faculty of Science, Chiang Mai University.

Radulae were extracted under a stereomicroscope, boiled with 10% sodium hydroxide for 5 min, washed with distilled water and observed under a stereomicroscope. Radulae were dehydrated by immersion in increasing concentrations of ethanol (10, 20, 30, 50, 70, 85 and 95%) before SEM, with each step taking 5 min (Yang and Zhang 2011). Radulae were mounted on aluminium stubs using carbon conductive adhesive tape, coated with gold and observed with an LV-Scanning Electron Microscope (JSM 5910 LV) as listed above.

### DNA extraction, amplification and sequencing

Genomic DNA of 21 specimens of *Anentome* aff. *wykoffi* was extracted from a small piece of the foot muscle tissue using 150  $\mu$ L of 5% of Chelex 100 and 3  $\mu$ L of Proteinase K. Samples were incubated at 55°C for 1 h, 95°C for 30 min and centrifuged at 11 336g at room temperature for 1 min. DNA extracted from the supernatant was stored at -20°C until use. A fragment of the mitochondrial cytochrome c oxidase subunit I (*COI*) gene and a fragment of the nuclear 28S rRNA gene were amplified by PCR using the primers LCOI490 (5'-GGT CAA CAA ATC ATA AAG ATA TTG G-3') and HCO2198 (5'-TAA ACT TCA GGG TGA CCA AAA AAT CA-3') for *COI* (Folmer et al. 1994), and C1 (5'-ACC CGC TGA ATT TAA GCA T-3') and D2 (5'-TCC GTG TTT CAA GAC GG-3') for 28S rRNA (Chisholm et al. 2001). PCR amplification was performed in reaction volumes of 20  $\mu$ L containing 10  $\mu$ L of 2 $\times$  Illustra Hot Start Master Mix (GE Healthcare), 1  $\mu$ L of each primer (10 mM), ~1 ng of DNA template and deionised water up to 20  $\mu$ L. For *COI*, thermal cycling

involved 94°C for 2 min, followed by 36 cycles of 94°C for 30 s, 42°C for 2 min and 72°C for 2 min, and a final extension step of 72°C for 5 min. For 28S rRNA, thermal cycling involved one cycle of 95°C for 3 min, 45°C for 2 min and 72°C for 90 s, followed by four cycles of 95°C for 45 s, 50°C for 45 s and 72°C for 90 s, in turn followed by 25 cycles of 95°C for 20 s, 52°C for 20 s and 72°C for 90 s and a final extension step of 72°C for 5 min. The amplicon size was checked by 1% (w/v) agarose gel electrophoresis using 1 $\times$  TBE buffer. Gels were run at 100 V for 20 min and visualised with RedSafe nucleic acid staining solution and UV transillumination. The PCR products were purified using the BigDye Terminator (ver. 3.1) cycle sequencing kit chemistry. The amplified PCR products were directly cycle-sequenced using the original amplification primers with the sequencing reaction products run on 1st BASE DNA Sequencing Services (Applied Biosystems).

### Phylogenetic analyses of DNA sequences

DNA sequences were edited and aligned with ClustalW (ver. 2, see <http://www.clustal.org/clustal2/>; Thompson et al. 1994) as implemented in MEGA (ver. 7, see <https://www.megasoftware.net/>; Kumar et al. 2016) and improved manually. *COI* sequences were checked for stop codons and frame-shift mutations. 28S rRNA sequences were used after complete deletion of missing-information and alignment gaps (indels). All new sequences were deposited in GenBank (Table 1).

Phylogenetic trees were inferred using neighbour-joining (NJ) (Saitou and Nei 1987), maximum likelihood (ML) (Sullivan 2005) and Bayesian inference (BI) (Ronquist et al. 2012). The genus *Nassarius* was used as an outgroup. The best-fit evolutionary substitution model based on the Akaike Information Criterion (Akaike 1974) as implemented in jModeltest2 (ver. 2.1.10, see <https://github.com/ddarriba/jmodeltest2>; Darriba et al. 2012) was GTR + I + G for the tree datasets: *COI*, 28S rRNA and the concatenated *COI*-28S alignment. NJ- trees were constructed and pairwise genetic distances based on the *COI* sequences were calculated using the Kimura 2-parameter model (K2P) (Kimura 1980) in MEGA (ver. 7; Kumar et al. 2016) with 1000 bootstrap replicates. ML-trees were constructed using PhyML (ver. 3, see <http://www.atgc-montpellier.fr/phyml/>; Guindon et al. 2009) with 1000 bootstrap replicates. Bootstrap values higher than 70% were considered to provide strong support (Hillis and Bull 1993). Bayesian inference was performed using MrBayes (ver. 3.2.7, see <https://nbisweden.github.io/MrBayes/index.html>; Ronquist et al. 2012). The Markov Chain Monte Carlo (MCMC) search was run with four chains for 7 000 000 generations with the heating parameter set at 0.09, tree sampling every 100 generations and burn-in set at 25%. Posterior probabilities were considered significant when  $\geq 0.95$  (San Mauro and Agorreta 2010). Tree topologies were drawn with FigTree (ver. 1.4.3, A. Rambaut, see <http://tree.bio.ed.ac.uk/software/figtree/>).

## Haplotype network analyses

*COI* haplotypes were analysed using DnaSP (ver. 6.12.03, see <http://www.ub.edu/dnasp/>; Rozas *et al.* 2017). A haplotype network was generated and visualised with the TCS method (Clement *et al.* 2000) as implemented in PopART (ver. 1.7, see <https://popart.maths.otago.ac.nz/>; Leigh and Bryant 2015). River drainage systems where the detected haplotypes of *A. wykoffi* were found (Table 1) were used as traits and employed in building the haplotype network (Yodsiri *et al.* 2017).

## Species delimitation

Species delimitation methods were applied to the *COI* and *28S* rRNA data using the (i) Assemble Species by Automatic Partitioning (ASAP) (Puillandre *et al.* 2021), (ii) generalised mixed Yule-Coalescent (GMYC) (Fujisawa and Barraclough 2013) and (iii) Bayesian Poisson tree processes (bPTP) (Zhang *et al.* 2013) methods.

ASAP was run on the web server (see <https://bioinfo.mnhn.fr/abi/public/asap/>) with the default settings and the K2P (Kimura 1980) substitution model.

The GMYC and bPTP methods require the input of an ultrametric tree from the BEAST package (ver. 1.10.4, see <https://beast.community/>; Suchard *et al.* 2018). An XML file was made with BEAUti (ver. 1.10.4, see <https://beast.community/beauti>) using the relaxed log-normal clock algorithm with the GTR + I + G model. The tree was reconstructed for  $1 \times 10^7$  generations with sampling every 1000 steps. The output tree was analysed with TreeAnnotator (ver. 1.10.4, see <https://beast.community/treeannotator>). The tree file was displayed in FigTree (ver. 1.4.3). GMYC was performed using both a single and multiple thresholds, and run on the web server (see <https://species.h-its.org/gmyc/>). bPTP was carried out on the bPTP web server (see <https://species.h-its.org/ptp/>).

## Results

### Sampling

In total, 125 specimens of *Anentome* aff. *wykoffi* were collected from 12 localities (Table 1, Fig. 1) in Thailand. The species seems to occur in at least five drainage systems in three river basins, viz. the Wang drainage in the Chao Phraya basin, the Chi, Mun and Mekong drainages in the middle Mekong basin, and the Tonle Sap drainage in the lower Mekong basin (Fig. 1). Based on the intraspecific variation we observed in *A. wykoffi*, we defined three putative morphotypes that could be distinguished by combining three characters: the presence or absence of a carinated shoulder, the number of spiral lines on the spira and the pattern of the central cusps on the central tooth of the radula.

## Morphological analysis

The one-way ANOVA (with Tukey's *post hoc* test for multiple comparisons) revealed that the shells of the three putative morphotypes differed significantly ( $P < 0.01$ ) from each other for 19 out of the 25 shell parameters studied (not AH, SH/SW, SW/AW, LWW/AW, SW/SCW and AW/SCW; Table 2).

In the geometric morphometric analysis, the CVA based on shell shape variation with the three putative morphotypes of *A. wykoffi* as *a priori* groups provided a graphic display of the shape differences based on the two CV variables obtained (Fig. 3a). CV1 explained 76.90% of the total variance in shape variation, with an eigenvalue of 0.9684 and CV2 explained the remaining 23.10% of the total variance in shape variation, with an eigenvalue of 0.2909. Overall, the shell shapes of the three putative morphotypes were rather well distinguished, even if these showed some overlap. This distinction was confirmed by the significant differences among the putative morphotypes as shown by the permutation tests of the Mahalanobis and Procrustes distances ( $P < 0.0001$ ).

The wireframe modifications in Fig. 3b describe the shell shape changes from the consensus configuration along the two CVs. Individuals located in the positive portion of the axis for CV1 had a narrower shell than individuals located in the negative portion. Individuals located in the negative portion of the axis for CV2 had a wider aperture than individuals located in the positive portion.

## Phylogenetic analyses of DNA sequences

Nucleotide sequences of the *COI* (657 bp), *28S* rRNA (728 bp) and concatenated dataset of the two fragments (1385 bp) were aligned, along with *Nassarius arcularia* and *N. boucheti* as outgroup taxa. Not unexpectedly, the trees based on the separate analyses of *COI* and *28S* rRNA were somewhat less well resolved but remained largely congruent or did not significantly contradict the concatenated analyses.

The NJ, ML and BI trees based on the concatenated dataset revealed that the four species of the genus *Anentome* (*A. cambojiensis*, *A. helena*, *A. costulata* and *A. wykoffi*) form a maximally supported clade in all analyses (Fig. 4).

The three morphotypes of *A. wykoffi* formed three well-supported clades, making *A. wykoffi* paraphyletic with the inclusion of *A. cambojiensis* (Fig. 4). Clade A (morphotype A) included mainly specimens from the Chi, Mun and Mekong drainages (localities 2–9). Clade B (morphotype B) included specimens from the Tonle Sap (locality 12) and Mun drainages (locality 10–11). Clade C (morphotype C) included specimens from the Wang drainage (locality 1) and formed a well-supported clade with *A. cambojiensis*.

The *COI* K2P-distances among *Anentome* species ranged from  $3.65 \pm 0.82$  to  $15.82 \pm 1.79\%$ . The K2P-distances among three clades of *A. wykoffi* ranged from  $3.74 \pm 0.75$  to  $7.17 \pm 0.98\%$ . The intraspecific K2P-distances within

**Table 2.** Shell morphometrics of three putative morphotypes of *A. wykoffi* examined in the present study.

Shell parameters	Morphotype A (n = 76) (mm)	Morphotype B (n = 33) (mm)	Morphotype C (n = 16) (mm)	F-value	P-value
SH	15.55 ± 2.28 <sup>a</sup> (11.28–20.88)	17.82 ± 1.68 <sup>b</sup> (14.91–22.41)	15.16 ± 2.56 <sup>a</sup> (9.37–19.72)	13.703	0.000*
SW	7.14 ± 0.99 <sup>a</sup> (5.33–9.22)	7.93 ± 0.55 <sup>b</sup> (7.10–9.83)	6.91 ± 0.98 <sup>a</sup> (4.86–8.32)	9.686	0.000*
AH	7.01 ± 1.00 <sup>a</sup> (5.13–9.13)	7.37 ± 0.56 <sup>a</sup> (6.20–9.16)	6.97 ± 1.02 <sup>a</sup> (4.76–8.35)	3.462	0.141
AW	3.64 ± 0.57 <sup>a</sup> (2.33–4.67)	4.02 ± 0.28 <sup>b</sup> (3.57–4.76)	3.56 ± 0.46 <sup>a</sup> (2.38–4.26)	6.957	0.001*
LWH	10.53 ± 1.52 <sup>ab</sup> (7.62–13.99)	11.37 ± 0.89 <sup>b</sup> (9.88–14.06)	10.28 ± 1.57 <sup>a</sup> (6.69–13.11)	4.999	0.008*
LWW	6.20 ± 0.79 <sup>a</sup> (4.56–7.63)	6.86 ± 0.45 <sup>b</sup> (6.13–8.46)	6.35 ± 0.78 <sup>a</sup> (4.48–7.72)	11.941	0.000*
SCW	1.73 ± 0.26 <sup>a</sup> (1.28–2.63)	1.93 ± 0.17 <sup>b</sup> (1.66–2.50)	1.63 ± 0.25 <sup>a</sup> (1.21–2.11)	8.170	0.000*
SH-LWH	5.02 ± 0.98 <sup>a</sup> (3.31–7.41)	6.45 ± 1.07 <sup>b</sup> (4.09–8.59)	4.88 ± 1.16 <sup>a</sup> (2.68–6.77)	23.786	0.000*
SPH	8.54 ± 1.36 <sup>a</sup> (6.15–11.75)	10.45 ± 1.34 <sup>b</sup> (7.70–13.39)	8.2 ± 1.64 <sup>a</sup> (4.61–11.38)	22.937	0.000*
SH/SW	2.18 ± 0.12 <sup>a</sup> (1.90–2.42)	2.25 ± 0.14 <sup>a</sup> (1.96–2.49)	2.19 ± 0.14 <sup>a</sup> (1.93–2.5)	3.624	0.035
AH/AW	1.93 ± 0.13 <sup>b</sup> (1.74–2.64)	1.83 ± 0.10 <sup>a</sup> (1.66–2.01)	1.95 ± 0.11 <sup>b</sup> (1.78–2.24)	11.770	0.000*
SH/AH	2.22 ± 0.09 <sup>a</sup> (2.02–2.42)	2.42 ± 0.17 <sup>b</sup> (2.07–2.85)	2.17 ± 0.13 <sup>a</sup> (1.97–2.47)	33.335	0.000*
SW/AW	1.97 ± 0.11 <sup>a</sup> (1.80–2.59)	1.97 ± 0.08 <sup>a</sup> (1.84–2.13)	1.94 ± 0.12 <sup>a</sup> (1.65–2.13)	0.119	0.564
SH/LWH	1.48 ± 0.07 <sup>a</sup> (1.33–1.68)	1.57 ± 0.09 <sup>b</sup> (1.37–1.75)	1.47 ± 0.08 <sup>a</sup> (1.36–1.65)	18.130	0.000*
LWH/(SH-LWH)	2.14 ± 0.32 <sup>b</sup> (1.48–3.07)	1.81 ± 0.31 <sup>a</sup> (1.34–2.68)	2.17 ± 0.33 <sup>b</sup> (1.53–2.77)	13.081	0.000*
LWH/AH	1.50 ± 0.05 <sup>a</sup> (1.35–1.59)	1.54 ± 0.05 <sup>b</sup> (1.44–1.67)	1.48 ± 0.07 <sup>a</sup> (1.33–1.6)	11.126	0.000*
SPH/AH	1.22 ± 0.09 <sup>a</sup> (1.02–1.42)	1.42 ± 0.17 <sup>b</sup> (1.07–1.85)	1.17 ± 0.13 <sup>a</sup> (0.97–1.47)	33.335	0.000*
SW/LWW	1.15 ± 0.04 <sup>b</sup> (1.06–1.28)	1.16 ± 0.04 <sup>b</sup> (1.08–1.23)	1.09 ± 0.04 <sup>a</sup> (0.98–1.13)	5.181	0.000*
LWW/AW	1.71 ± 0.12 <sup>a</sup> (1.49–2.36)	1.71 ± 0.09 <sup>a</sup> (1.55–1.87)	1.79 ± 0.08 <sup>b</sup> (1.66–1.94)	2.057	0.039
SW/SCW	4.14 ± 0.37 <sup>a</sup> (3.25–5.02)	4.11 ± 0.25 <sup>a</sup> (3.61–4.57)	4.25 ± 0.36 <sup>a</sup> (3.74–5.25)	0.941	0.392
AW/SCW	2.11 ± 0.21 <sup>a</sup> (1.64–2.63)	2.09 ± 0.16 <sup>a</sup> (1.73–2.45)	2.20 ± 0.24 <sup>a</sup> (1.88–2.89)	0.538	0.182
LWW/SCW	3.60 ± 0.33 <sup>a</sup> (2.80–4.38)	3.56 ± 0.23 <sup>a</sup> (3.02–4.14)	3.92 ± 0.30 <sup>b</sup> (3.63–4.82)	3.543	0.000*
LWH/SH	0.68 ± 0.03 <sup>b</sup> (0.60–0.76)	0.64 ± 0.04 <sup>a</sup> (0.57–0.73)	0.68 ± 0.03 <sup>b</sup> (0.61–0.74)	16.532	0.000*
AH/SH	0.45 ± 0.02 <sup>b</sup> (0.41–0.50)	0.42 ± 0.03 <sup>a</sup> (0.35–0.48)	0.46 ± 0.03 <sup>b</sup> (0.41–0.51)	31.961	0.000*
SPH/SH	0.55 ± 0.02 <sup>a</sup> (0.51–0.59)	0.58 ± 0.03 <sup>b</sup> (0.52–0.65)	0.54 ± 0.03 <sup>a</sup> (0.49–0.60)	30.993	0.000*

Morphotype measurements are mean ± s.d. value (minimum–maximum). n, number of adult shells examined. Superscript lowercase letter (a, b and c) indicate test results of Tukey's *post hoc* test from one-way ANOVA for differences among putative morphotypes (parameter measurements with shared superscripts are not significantly different ( $P < 0.01$ ) from each other). Probabilities are significant at: \*,  $P < 0.01$ .

*A. wykoffi* clades A, B and C were  $1.82 \pm 0.31$ ,  $0.10 \pm 0.13$  and  $0.00 \pm 0.00\%$  respectively (Table 3).

### Haplotype network analysis

The TCS haplotype network of *COI* sequences (Fig. 5) suggests three haplogroups that correspond with the three putative morphotypes A, B and C. Haplogroup A comprises 11 haplotypes (Hap1–11) from the Chi, Mun and Mekong drainages (localities 2–9), with hap1 and hap2 being somewhat differentiated from the other A group haplotypes by 11 mutational steps. Haplogroup A differs from haplogroups B and C by 27 and 41 mutational steps respectively. Haplogroup B comprises hap12 (Mun drainage; localities 10 and 11) and hap13 (Tonle Sap drainage; locality 12)

that are separated by only two mutational steps. Haplogroup C only comprises hap14 (Wang drainage; locality 1) that differs from haplogroup B in 28 mutational steps.

### Species delimitation

The three species delimitation methods (ASAP, GMYC and bPTP) based on *COI* sequences consistently suggested that the three clades originally identified as *A. wykoffi* represent putative species, coinciding with morphotypes A, B and C. These are supported by morphological characteristics and can be distinguished by the carinated shoulder, number of spiral lines on the spira and pattern of the central cusps on the central tooth of the radula (Fig. 6). However, both GMYC and bPTP further subdivided clade A into three

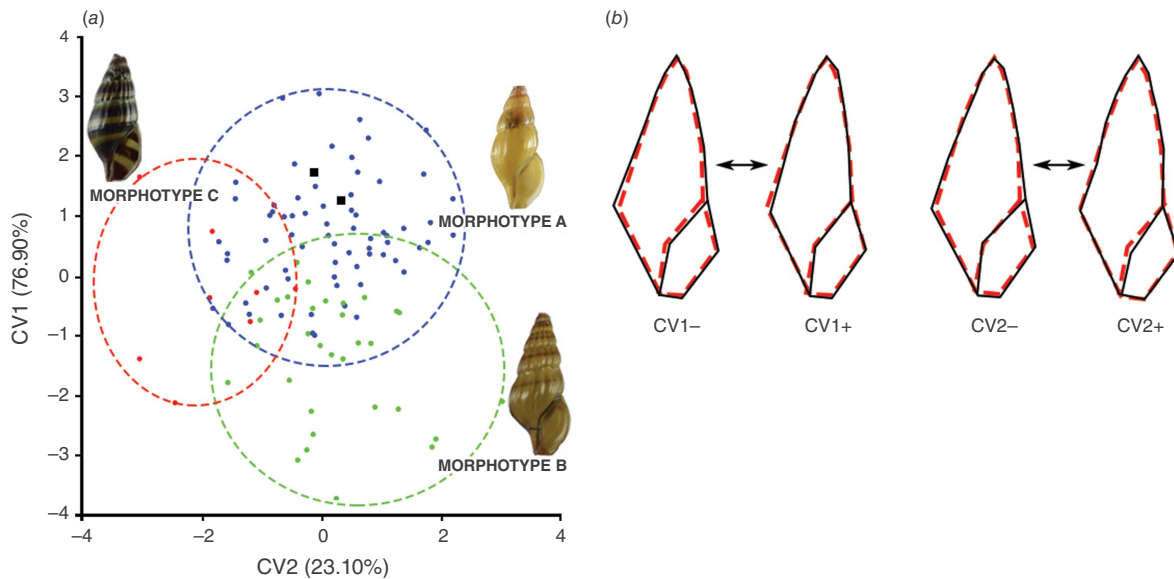


**Fig. 3.** Geometric morphometric study of shell shape variation in *A. wykoffi*. (a) Plots of individual scores for the canonical variates (CVs) that were derived from the canonical variate analysis (CVA); blue, green and red circles represent individuals with morphotypes a, b and c respectively, and black squares represent the type specimens of *A. wykoffi* (Holotype SMF 219824 and Paratype SMF 225241). (b) Wireframe modifications derived from the CVA showing the shell shape changes (black solid line) from the consensus configuration (red dashed line) in relation to each of the negative and positive portions of the CVs. Shape changes along CV1 are shown on the left and those along CV2 on the right.

putative species (A-1, A-2 and A-3; Fig. 6). Yet these three putative species showed very limited *COI* sequence divergence (1.82%) and appeared morphologically indistinguishable, therefore we did not retain these for taxonomic treatment. Besides, ASAP and GMYC for 28S rRNA sequences failed to separate the three clades of *A. wykoffi* into three putative species. Conversely, the three morphotypes and *COI*-28S rRNA clades are proposed to be different species, two of which are new to science.

## Systematics

### Family NASSARIIDAE Iredale, 1916 (1835)

### Genus *Anentome* Cossmann, 1901

### *Anentome wykoffi* (Brandt, 1974) (*sensu stricto*)

(Fig. 4, clade A, and 7a, b, e, h.)

ZooBank: [urn:lsid:zoobank.org:act:3307039C-6327-42CB-9E62-A2E600873001](https://www.zoobank.org/urn:lsid:zoobank.org:act:3307039C-6327-42CB-9E62-A2E600873001)

*Clea (Anentome) wykoffi* Brandt, 1974, p. 204, pl. 15, fig. 69. *Type locality*: Mekong at Bandan in Thailand.

*Clea wykoffi* (Brandt, 1974) – Kittivorachate and Yangyuen (2004), p. 133, Ubol Ratana Dam, Khon Kaen, Thailand.

*Anentome wykoffi* (Brandt, 1974) – Chomchoei *et al.* (2022), table 1, fig. 1, Ban Kong, Nong Ruea, Khon Kaen, Thailand; Khemmarat, Ubon Ratchathani, Thailand; Khong Chiam, Ubon Ratchathani, Thailand.

## Material examined

### Type material

**Holotype.** SMF 219824 (Fig. 7a) and Paratype SMF 225241 from Mekong at Bandan in Thailand. Non-type material: **THAILAND:** Ubol Ratana Dam, Khon Kaen: CMUZ A213003 (1 shell) and CMUZ A213031 (3 specimens in  $-20^{\circ}\text{C}$ ), Huai Kut Daeng Reservoir, Roi Ed: CMUZ A193004 (1 shell), CMUZ A193005 (1 shell) and CMUZ A193032 (5 specimens in  $-20^{\circ}\text{C}$ ), Phaya Thaen Public Park, Yasothorn: CMUZ A193006 (1 shell), CMUZ A193007 (1 shell), CMUZ A193029 (1 shell), CMUZ A193030 (1 shell) and CMUZ A193033 (8 specimens in  $-20^{\circ}\text{C}$ ), Mekong River, Khemmarat, Ubon Ratchathani: CMUZ A213013 (1 shell) and CMUZ A213034 (8 specimens in  $-20^{\circ}\text{C}$ ), Wat Ban Dan, Ubon Ratchathani: CMUZ A213014 (1 shell), CMUZ A213015 (1 shell; Fig. 7b), CMUZ A213016 (1 shell) and CMUZ A213035 (7 specimens in  $-20^{\circ}\text{C}$ ), Mun River Bridge, Khong Chiam, Ubon Ratchathani: CMUZ A213008 (1 shell), CMUZ A213009 (1 shell) and CMUZ A213036 (8 specimens in  $-20^{\circ}\text{C}$ ), Sirindhorn Dam, Ubon Ratchathani: CMUZ A193010 (1 shell), CMUZ A193011 (1 shell) and CMUZ A193037 (11 specimens in  $-20^{\circ}\text{C}$ ), Lam Dom Noi, Ubon Ratchathani: CMUZ A213012 (1 shell) and CMUZ A213038 (2 specimens in  $-20^{\circ}\text{C}$ ).

## Description

### Shell (Fig. 7b, e) ( $n = 76$ )

Shell fusiform, ovate-conoidal, solid. Apex typically eroded. Whorls 5, well rounded. Suture convex and deep. Shell longitudinally ribbed, 14–22 axial ribs on the last whorl, equally strong and evenly spaced. Spiral lines, grow coarser at the base of the body whorl, cross the axial ribs, 3–5 thin spiral lines on the spira. Aperture oval, angled above and protracted below, outer lip thin. Siphonal canal short and broad. The last whorl height to shell height  $\sim 2/3$

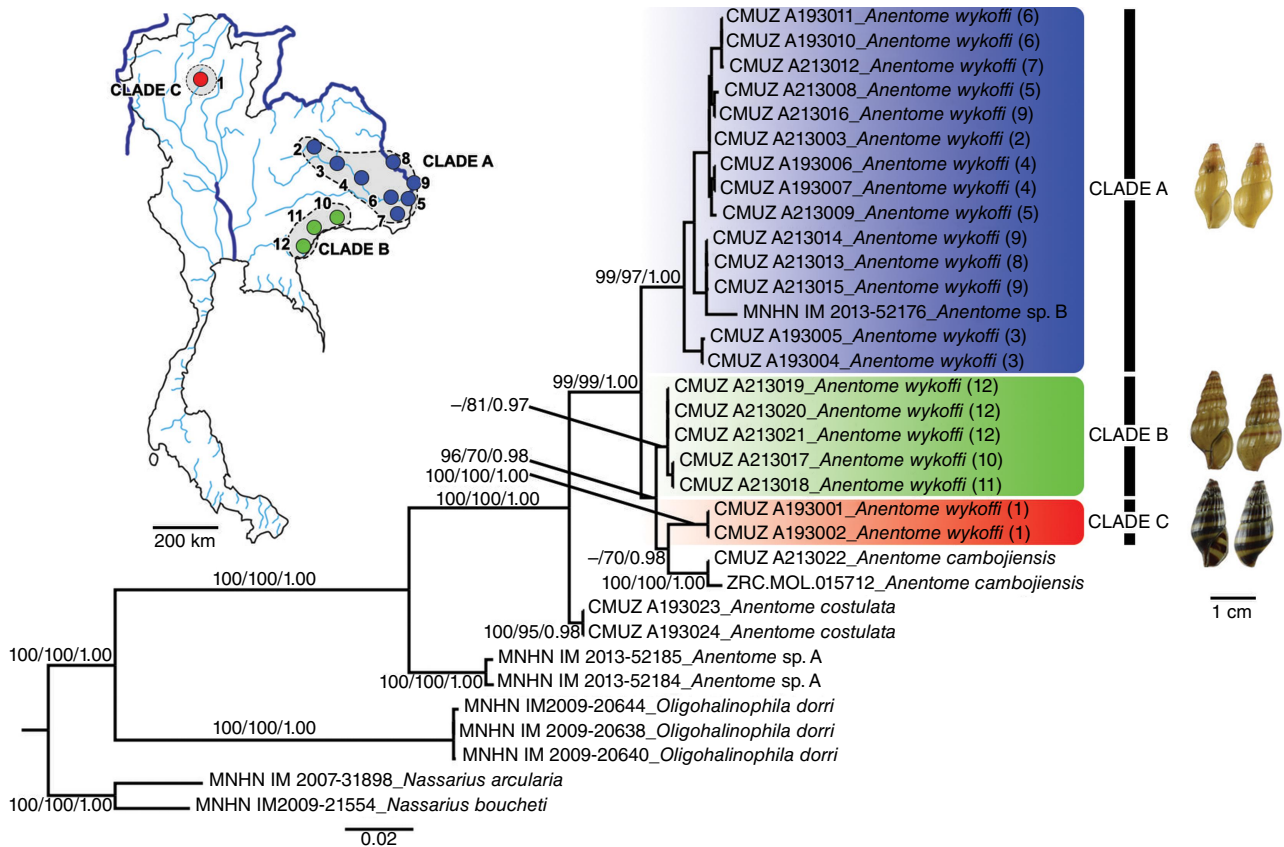


**Fig. 4.** BI tree of *A. wykoffi* and related species based on 1385 nucleotide sites in a concatenated *COI* (657 bp) and 28S rRNA (728 bp) alignment. Numbers at the branches are NJ bootstrap (BP)/ML bootstrap (BP)/BI posterior probability (PP) values. The map shows the sampling localities (numbered from 1 to 12 in both the map and the phylogenetic tree) with their morphotypes (clade colours).

**Table 3.** Mean *COI* divergences (K2P model: percentage ± standard error) among the *Anentome* spp. taxa included in the phylogenetic tree of Fig. 4.

<i>Anentome</i> spp.	1	2	3	4	5	6
1 <i>A. wykoffi</i> clade A	<b>1.82 ± 0.31</b>					
2 <i>A. wykoffi</i> clade B	4.95 ± 0.77	<b>0.10 ± 0.13</b>				
3 <i>A. wykoffi</i> clade C	7.17 ± 0.98	3.74 ± 0.75	<b>0.00 ± 0.00</b>			
4 <i>A. cambojiensis</i>	6.76 ± 1.08	3.65 ± 0.82	4.73 ± 0.89	<b>0.64 ± 0.43</b>		
5 <i>A. costulata</i>	7.30 ± 1.01	5.64 ± 0.96	6.57 ± 1.07	7.19 ± 2.04	<b>0.00 ± 0.00</b>	
6 <i>Anentome</i> sp. A	14.18 ± 1.58	13.84 ± 1.62	15.82 ± 1.79	14.83 ± 1.21	11.24 ± 1.44	<b>0.22 ± 0.22</b>

Average intraspecific distances within each taxon are shown in bold.

(0.7) and apertural height to shell height ~1/2 (0.5). Spira height up to 11.7 mm and spira height to shell height ~1/2 (0.5). Shell colour olive, brownish or yellowish, 1–3 dark or light brown bands on each whorl or no bands. Operculum almond-shaped, concentric, corneous, with basal nucleus.

**Radula (Fig. 7h) (n = 30)**

Stenoglossan radula, 3 teeth on each row with formula 1-1-1. Central tooth evenly arched, posterior margin with 5–9 long, sharply pointed cusps, all cusps are similar in size

(except towards the sides where these tend to become smaller). Lateral teeth typically tricuspid, occasionally with a fourth cusp; the central cusp much narrower and closer to the inner cusp, and the outer cusp sharply pointed with C shape, larger than the central and inner cusps.

**Remarks**

*Anentome wykoffi* is conchologically very similar to *A. cambojiensis*, *A. helena*, *A. longispira* sp. nov. and

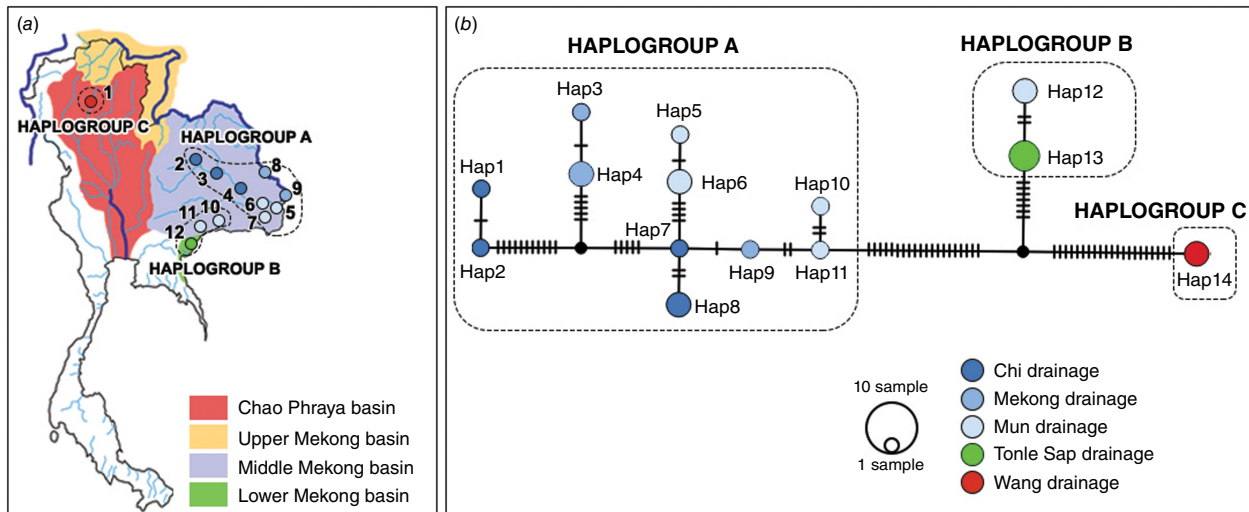


**Fig. 5.** (a) Distribution of the haplotypes of *A. wykoffi* in the different drainage systems in Thailand (the numbers in the map are the locality numbers). (b) TCS network of *COI* haplotypes of *A. wykoffi*. Drainage systems are indicated by different colours. Circles of different sizes represent the number of individuals with a given haplotype. Hatch marks along the branches indicate the numbers of mutational steps and black dots represent hypothetical haplotypes (Hap, haplotype).

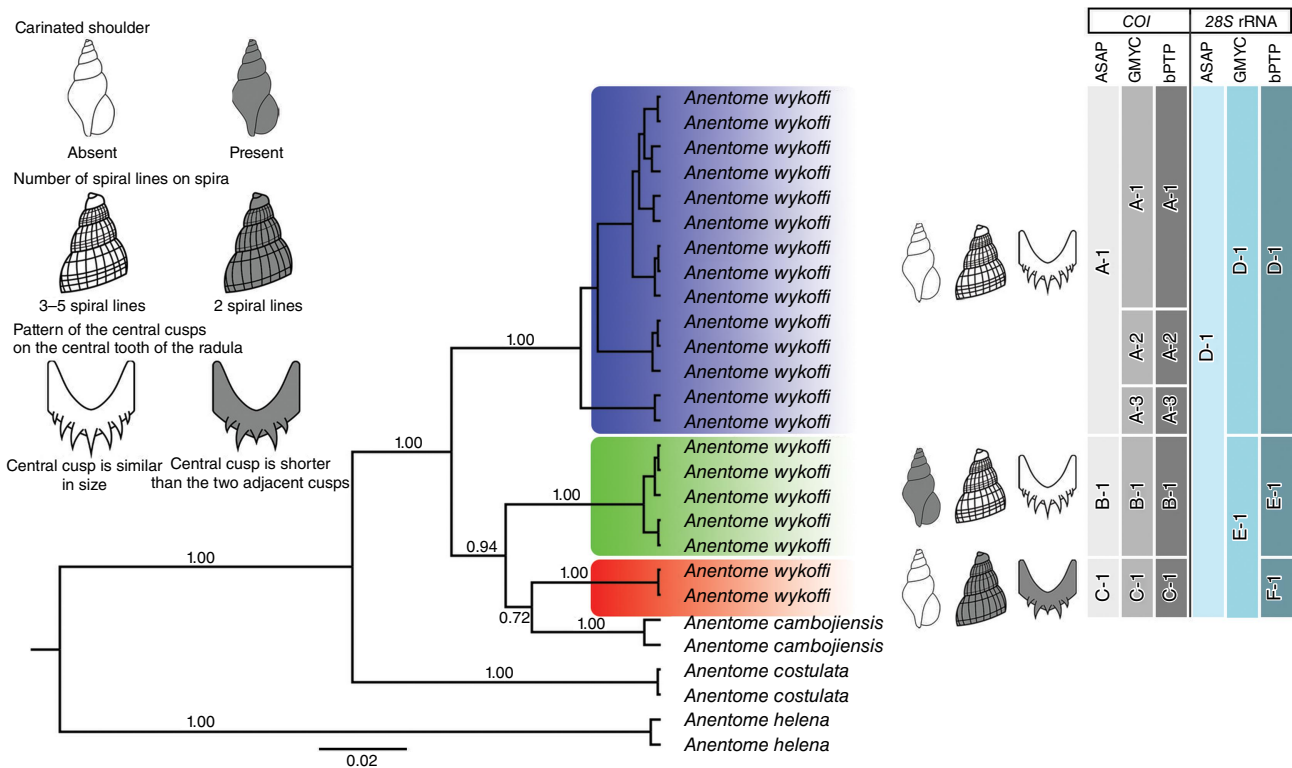


**Fig. 6.** Species delimitation analyses of *A. wykoffi* based on *COI* and 28S rRNA sequences using ASAP, GMYC and bPTP. The putative species are labelled with letters and numbers. Posterior probabilities of the BI tree are provided at the branches. The upper left part of the figure provides a synopsis of three morphological characters by which the three morphotypes are primarily defined: (1) carinated shoulder, (2) number of spiral lines on spira, and (3) pattern of the central cusps on the central tooth of the radula.

*A. khelangensis* sp. nov. However, the species can be distinguished as follows: *A. cambojiensis* has 5 whorls and whorls well-rounded, not inflated and tubercled at the angle of the

whorls; *A. helena* has 5 whorls, whorls well-rounded, narrower costulation, thinner texture and shorter siphonal canal (Brandt 1974); *A. longispira* sp. nov. has well-rounded whorls

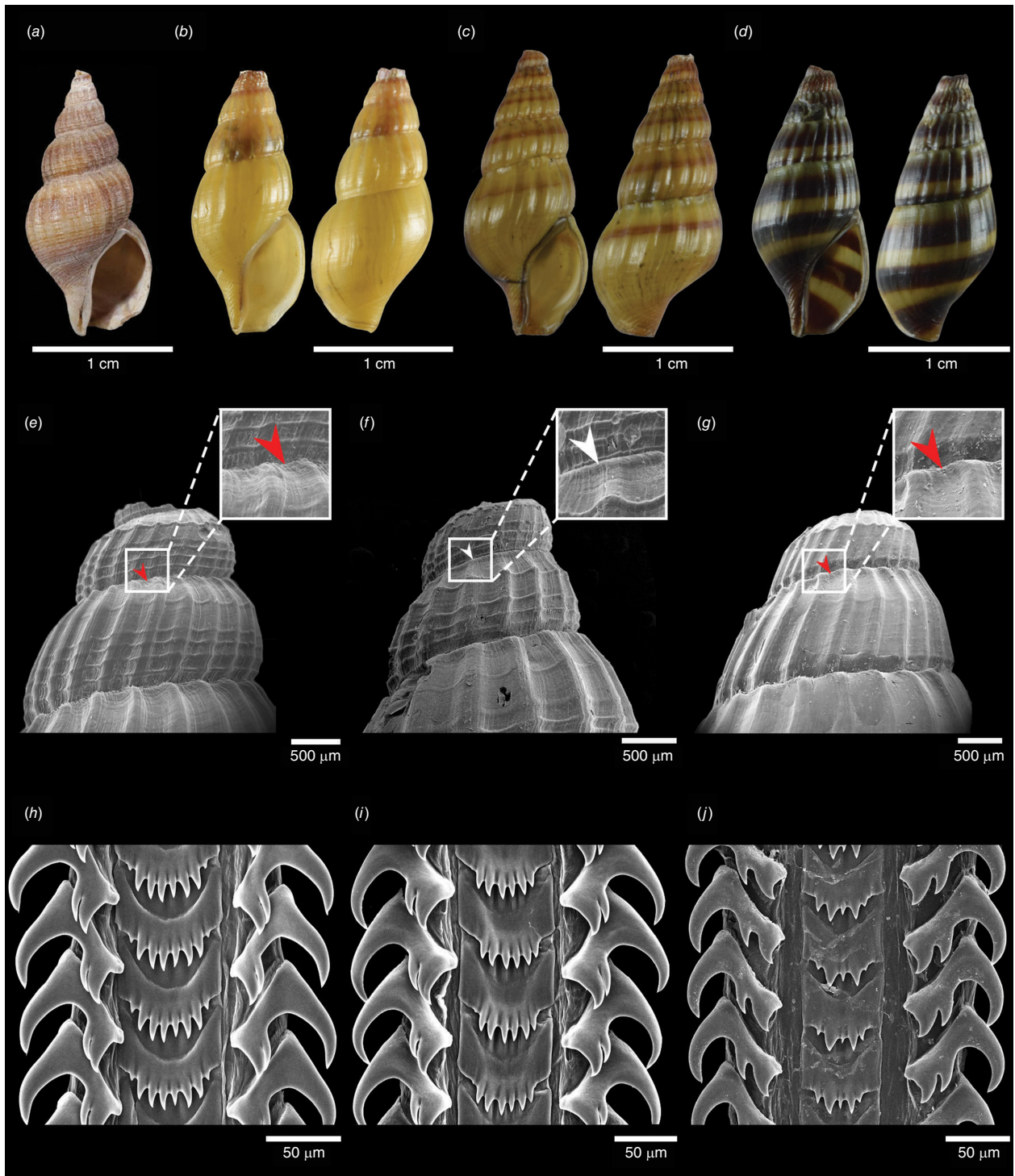


**Fig. 7.** Morphological comparison of species formerly grouped under the name *Anentome wykoffi*. (a) *A. wykoffi* holotype SMF 219824, (b) *A. wykoffi* CMUZ A213015 (Clade A in Fig. 4), (c) *A. longispira* sp. nov. (Clade B in Fig. 4) holotype CMUZ A213021, and (d) *A. khelangensis* sp. nov. (Clade C in Fig. 4) holotype CMUZ A193001. SEM images of the shell apex (e–g) and radula (h–j) of *A. wykoffi* (clade A) (e, h), *A. longispira* sp. nov. (clade B) (f, i) and *A. khelangensis* sp. nov. (clade C) (g, j) (white arrow: the carinated shoulder present; red arrow: the carinated shoulder absent).

that are not carinated (Fig. 7); and *A. khelangensis* sp. nov. has 3–5 spiral lines on the spira, and the central cusps on the central tooth of the radula are similar in size (Fig. 7).

***Anentome longispira* Chomchoei & Nantarat,  
sp. nov.**

(Fig. 4, clade B, and 7c, f, i.)

ZooBank: [urn:lsid:zoobank.org:act:7FF63177-8938-4E8C-8085-08A4D8CA6BE8](http://urn:lsid:zoobank.org:act:7FF63177-8938-4E8C-8085-08A4D8CA6BE8)

*Anentome wykoffi* (Brandt, 1974) – Chomchoei *et al.* (2022), table 1, fig. 1, Dan, Kap Choeng, Surin, Thailand; Non Din Daeng, Buri Ram, Thailand; Aranyaprathet, Aranyaprathet, Sa Kaeo, Thailand.

### Material examined

#### Type material

**Holotype.** CMUZ A213021 (Fig. 7c; shell height 22.41 mm, shell width 9.83 mm). Paratypes CMUZ A213019 (1 shell), CMUZ A213020 (1 shell), CMUZ A213028 (1 shell) and CMUZ A213039 (26 specimens in  $-20^{\circ}\text{C}$ ). Non-type material: **THAILAND:** Huai Dan Reservoir, Surin: CMUZ A213017 (1 shells) and CMUZ A213040 (2 specimens in  $-20^{\circ}\text{C}$ ), Lam Nang Rong Dam, Buri Ram: CMUZ A213018 (1 shell) and CMUZ A213041 (1 specimen in  $-20^{\circ}\text{C}$ ).

### GenBank accession numbers

Holotype CMUZ A213021: OP955882 (COI) and OP955908 (28S). Paratypes CMUZ A213019: OP955880 (COI) and OP955906 (28S), and CMUZ A213020: OP955881 (COI) and OP955907 (28S).

### Type locality

Huai Phrom Hot, Aranyaprathet District, Sa Kaeo Province (13°40'05.6"N; 102°31'24.8"E).

### Etymology

The specific epithet '*longispira*' (Latin for 'long spire') refers to the relatively long spira of this species.

### Description

#### Shell (Fig. 7c, f) ( $n = 33$ )

Shell fusiform, ovate–conoidal, solid. Apex typically eroded. Whorls 5, well rounded and carinated shoulder. Suture convex and deep. Shell longitudinally ribbed, 18–20 axial ribs on the last whorl, equally strong and evenly spaced. Spiral lines, grow coarser at the base of the body whorl, cross the axial ribs, 3–5 thin spiral lines on the spira. Aperture oval, angled above and protracted below, outer lip slightly thickened. Siphonal canal short but distinct. The last whorl height to shell height less than 2/3 (0.7) and apertural height to shell height less than 1/2 (0.5). Spira height up to 13.4 mm and spira height to shell height more than 1/2

(0.5). Shell colour olive, brownish or yellowish, 1–3 dark or light brown bands on each whorl. Operculum almond-shaped, concentric, corneous, with basal nucleus.

#### Radula (Fig. 7i) ( $n = 30$ )

Stenoglossan radula, 3 teeth on each row with formula 1-1-1. Central tooth evenly arched, posterior margin with 6–8 long, sharply pointed cusps, all cusps are similar in size (except towards the sides where these tend to become smaller). Lateral teeth typically tricuspid; the central cusp much narrower and closer to the inner cusp and the outer cusp, sharply pointed with C shape, larger than the central and inner cusps.

### Differential diagnosis

*Anentome longispira* sp. nov. differs from *A. wykoffi* and *A. khelangensis* sp. nov. in having a carinated shoulder, and from *A. khelangensis* sp. nov. in having 3–5 spiral lines on the spira. The spira of *A. longispira* sp. nov. is relatively longer than in *A. wykoffi* and *A. khelangensis* sp. nov. (Fig. 7). *Anentome longispira* sp. nov. was supported as clade B in the phylogenetic tree (Fig. 4) and the geometric morphometric analysis (Fig. 3). This species is known from Sa Kaeo, Buriram and Surin provinces. Based on our morphological and DNA sequence analyses, we suggest that *A. wykoffi* in Chomchoei *et al.* (2022) involves *A. longispira* sp. nov.

### Remarks

This species is distributed in a narrow area in eastern Thailand. The landscape includes low-lying plains, the Mekong Delta, mountains and the coastline of the Gulf of Thailand. The type locality borders the provinces Banteay Meanchey and Battambang in Cambodia.

***Anentome khelangensis* Chomchoei & Nantarat,  
sp. nov.**

(Fig. 4, clade C, and 7d, g, j.)

ZooBank: [urn:lsid:zoobank.org:act:72E73AF2-5CEA-44DD-A6CA-E5A90F798DD0](http://urn:lsid:zoobank.org:act:72E73AF2-5CEA-44DD-A6CA-E5A90F798DD0)

### Material examined

#### Type material

**Holotype.** CMUZ A193001 (Fig. 7d; shell height 19.72 mm, shell width 8.30 mm). Paratypes CMUZ A193002 (1 shell), CMUZ A193027 (1 shell) and CMUZ A193042 (13 specimens  $-20^{\circ}\text{C}$ ).

### GenBank accession numbers

Holotype CMUZ A193001: OP955862 (COI) and OP955888 (28S). Paratype CMUZ A193002: OP955863 (COI) and OP955889 (28S).

## Type locality

Huai Mae Nueang, Mueang Pan District, Lampang Province (18°32'04.0"N; 99°28'26.8"E), Thailand.

## Etymology

The specific epithet '*khelangensis*' refers to Khelang, a former name of Lampang Province, where the type locality is situated.

## Description

### Shell (Fig. 7d, g) (n = 16)

Shell fusiform, ovate-conoidal, solid. Apex typically eroded. Whorls 5, well rounded. Suture convex and deep. Shell longitudinally ribbed, 20–22 axial ribs on last whorl, moderately weak. Spiral lines grow coarser at the base of the body whorl and cross the axial ribs, 2 thin spiral lines on the spira. Aperture oval, angled above and protracted below, outer lip thin, Siphonal canal short but distinct. The last whorl height to shell height  $\sim 2/3$  (0.7) and apertural height to shell height  $\sim 1/2$  (0.5). Spira height up to 11.4 mm and spira height to shell height  $\sim 1/2$  (0.5). Shell brownish or yellowish, 1–3 dark brown bands on each whorl. Operculum almond-shaped, concentric, corneous with basal nucleus.

### Radula (Fig. 7j) (n = 10)

Stenoglossan radula, 3 teeth on each row with formula 1-1-1. Central tooth evenly arched, posterior margin with 5–7 long, sharply pointed denticles, central cusp is shorter than two adjacent cusps. Lateral teeth typically tricuspid; the central cusp much narrower and closer to the inner cusp and the outer cusp, sharply pointed with C shape, larger than the central and inner cusps.

## Differential diagnosis

*Anentome khelangensis* sp. nov. differs from *A. wykoffi* and *A. longispira* sp. nov. in having 2 spiral lines on the spira, and in the central cusp of the central tooth of the radula being shorter than the two adjacent cusps. This species differs from *A. cambojiensis* in the well rounded whorls that are not inflated and tubercled at the angle of the whorls, and in having 5 instead of 6 whorls. *Anentome khelangensis* sp. nov. was supported as clade C in the phylogenetic tree (Fig. 4) and the geometric morphometric analysis (Fig. 3).

## Remarks

This species is only known from the type locality in Lampang Province, Thailand.

## Discussion

Brandt (1974) described *A. wykoffi* based on a few dead shells from 'Mekong at Bandan in E Thailand' (Ubon

Ratchathani) in the Middle Mekong basin. Subsequently, Kittivorachate and Yangyuen (2004) reported the species from Ubol Rattana Dam, some 300 km west of the type locality but still in the Middle Mekong basin. Our current data show that *A. wykoffi* is far more widespread and common in the Middle Mekong basin than has been assumed, whereas the two putative new species further extend the range of the species complex to the Chao Phraya and Lower Mekong basins. However, the distribution of the species in the central and southern parts of the Chao Phraya basin remains to be investigated and the potential occurrence of the species in the Cambodian part of the Lower Mekong basin needs to be explored.

Starting from a preliminary distinction of three cryptic shell morphotypes within *Anentome wykoffi*, we demonstrated that these morphotypes show consistent morphometric and shell shape differences that correlate well with differences in shell sculpture and radula. The three morphotypes are also well separated by a phylogenetic analysis of *COI* and *28S* rRNA sequences, appearing as three well-supported clades that were recognised as putative cryptic species by three species delimitation methods. The three putative species seem to have separate, non-overlapping distributions. Consequently, although one of the putative species coincides with *A. wykoffi* (Brandt 1974) *sensu stricto* (morphotype A; distributed in the Middle Mekong basin), the other two putative species described here are new to science, namely, *A. longispira* sp. nov. (morphotype B; distributed in the Middle and Lower Mekong basin) and *A. khelangensis* sp. nov. (morphotype C; restricted to the Chao Phraya basin) (Fig. 3–7).

The intraspecific K2P *COI* divergences in the three putative species ranged from 0 to 1.82%, whereas the interspecific *COI* divergences ranged from 3.74 to 7.17%. These results are consistent with those for other Neogastropoda (particularly Nassariidae) that have intraspecific *COI* divergences ranging from 0 to 3.00% and interspecific *COI* divergences ranging from 2.10 to 19.80% (Zou et al. 2011; Galindo et al. 2017; Nerurkar et al. 2020). As a result, the levels of sequence divergence among the three putative species are approximately comparable to species-level divergences in other neogastropod and nassariid genera.

The species delimitation analyses based on the *COI* sequences supported the three clades from the phylogenetic trees (Fig. 4 and 5) and suggested three (ASAP) or five (GMYC and bPTP) possible species (Fig. 6). However, GMYC and bPTP sometimes overestimate numbers of putative species because of factors other than speciation (e.g. Dellicour and Flot 2018), and the additional putative species suggested in clade A by GMYC and bPTP were morphologically indistinguishable, therefore we currently adhere to a more conservative three-species interpretation. This conservative approach is consistent with the species delimitation results for *28S* rRNA, where ASAP did not separate clades A, B and C as putative species (Fig. 6), whereas GMYC suggested two putative species (clade A v.

clades B + C), resulting in only bPTP suggesting that the three species be retained from the COI analysis. Finally, the fact that *A. cambojiensis* appeared as a sister taxon to clade C (*A. khelangensis* sp. nov.), thereby making the former concept of *A. wykoffi* a paraphyletic taxon, reinforces the species level interpretation of the three *A. wykoffi* clades (morphotypes) distinguished here.

Given the morphological and phylogenetic analyses used in this work, the three cryptic species are to be interpreted as such under the morphological and phylogenetic species concepts. To what extent these are also reproductively isolated and hence represent biological species remains to be corroborated, even if the morphological data and 28S rRNA sequences presented here would traditionally be taken as evidence of reproductive isolation (i.e. biological species). Irrespective of the species concepts used, this study clearly confirms the earlier work of Strong *et al.* (2017) and Chomchoei *et al.* (2018) that showed that the genus *Anentome* is taxonomically far more diverse than had previously been assumed and hence needs revision. In this context, we provisionally followed current practice (e.g. Brandt 1974) by applying the name *A. helena* to *Anentome* specimens that are common in Thailand (Brandt 1974) and that form a well-supported clade with species A (from Phuket, Thailand) of Strong *et al.* (2017). However, the type locality of *A. helena* is 'Insula Java' (von dem Busch 1847), therefore the Thai material may well be considered to represent another species and may therefore need another name. Similarly, the present work shows that the use of the name '*A. wykoffi*' in some previous papers must be corrected. This applies to *A. wykoffi* in Chomchoei *et al.* (2022) that actually refers to *A. longispira* sp. nov., whereas species B in Strong *et al.* (2017) is *A. wykoffi* s.s. These taxonomic and nomenclatural changes are important for correctly diagnosing cryptic *Anentome* taxa that act as intermediate hosts of various trematode parasites or that are sold in the worldwide aquarium trade through which these parasites may be spread (e.g. Stanicka *et al.* 2022). At the same time, this type of taxonomic information is also necessary for the conservation of freshwater snails, especially in some parts of the Mekong drainages in Thailand, where freshwater snail populations have declined dramatically (Köhler *et al.* 2010).

## References

Adams A (1855) Description of two new genera and several new species of Mollusca, from the collection of Hugh Cuming Esq. *Proceedings of the Zoological Society of London* **23**, 119–124.

Akaike H (1974) A new look at the statistical model identification. *IEEE Transactions on Automatic Control* **19**, 716–723. doi:10.1109/TAC.1974.1100705

Brandt RAM (1974) The non-marine aquatic Mollusca of Thailand. *Archiv für Molluskenkunde* **105**, 1–423.

Butboonchoo P, Wongsawad C, Wongsawad P, Chai JY (2020) Morphology and molecular identification of *Echinostoma revolutum* and *Echinostoma macrorchis* in freshwater snails and experimental hamsters in upper northern Thailand. *The Korean Journal of Parasitology* **58**, 499–511. doi:10.3347/kjp.2020.58.5.499

Chantima K, Chai JY, Wongsawad C (2013) *Echinostoma revolutum*: freshwater snails as the second intermediate hosts in Chiang Mai, Thailand. *The Korean Journal of Parasitology* **51**, 183–189. doi:10.3347/kjp.2013.51.2.183

Chantima K, Suk-Ueng K, Kampan M (2018) Freshwater snail diversity in Mae Lao agricultural basin (Chiang Rai, Thailand) with a focus on larval trematode infections. *The Korean Journal of Parasitology* **56**, 247–257. doi:10.3347/kjp.2018.56.3.247

Chisholm LA, Morgan JAT, Adlard RD, Whittington ID (2001) Phylogenetic analysis of the Monocotylidae (Monogenea) inferred from 28S rDNA sequences. *International Journal for Parasitology* **31**, 1537–1547. doi:10.1016/S0020-7519(01)00313-7

Chomchoei N, Wongsawad C, Nantarat N (2018) Investigation of cryptic diversity and occurrence of echinostome metacercariae infection in *Anentome helena* (von dem Busch, 1847). *Asian Pacific Journal of Tropical Medicine* **11**, 590–596. doi:10.4103/1995-7645.244524

Chomchoei N, Bäckeljaun T, Segers B, Wongsawad C, Butboonchoo P, Nantarat N (2022) Morphological and molecular characterization of larval trematodes infecting the assassin snail genus *Anentome* in Thailand. *Journal of Helminthology* **96**, E52. doi:10.1017/S0022149X22000463

Clement M, Posada D, Crandall KA (2000) TCS: a computer program to estimate gene genealogies. *Molecular Ecology* **9**, 1657–1659. doi:10.1046/j.1365-294X.2000.01020.x

Coppo G, De Vos L (1986) Two different striation patterns of the protoconch in Galapagos Bulimulidae: an SEM study. *Journal of Molluscan Studies* **52**, 106–109. doi:10.1093/mollus/52.2.106

Cossmann AE (1901) 'Essais de Palé oconchologie comparée. Vol. 4. Paris.' (The Author and Société d'Éditions Scientifiques) [In French]

Darriba D, Taboada GL, Doallo R, Posada D (2012) jModelTest 2: more models, new heuristics and parallel computing. *Nature Methods* **9**, 772. doi:10.1038/nmeth.2109

Dellicour S, Flot JF (2018) The hitchhiker's guide to single-locus species delimitation. *Molecular Ecology Resources* **18**, 1234–1246. doi:10.1111/1755-0998.12908

Folmer O, Black M, Hoeh W, Lutz R, Vrijenhoek R (1994) DNA primers for amplification of mitochondrial cytochrome c oxidase subunit I from diverse metazoan invertebrates. *Molecular Marine Biology and Biotechnology* **3**, 294–299.

Food and Agriculture Organization of the United Nations (2021) Graphic overview: hydrological basins in Asia. Available at <https://data.apps.fao.org/catalog/dataset/ee616dc4-3118-4d67-ba05-6e93dd3e962f/resource/14e02901-31b4-4eef-bd48-e848e459a6be>

Fujisawa T, Barraclough TG (2013) Delimiting species using single-locus data and the generalized mixed yule coalescent approach: a revised method and evaluation on simulated data sets. *Systematic Biology* **62**, 707–724. doi:10.1093/sysbio/syt033

Galindo LA, Puillandre N, Utge J, Lozouet P, Bouchet P (2016) The phylogeny and systematics of the Nassariidae revisited (Gastropoda, Buccinoidea). *Molecular Phylogenetics and Evolution* **99**, 337–353. doi:10.1016/j.ympev.2016.03.019

Galindo LA, Kool HH, Dekker H (2017) Review of the *Nassarius pauperus* (Gould, 1850) complex (Nassariidae): part 3, reinstatement of the genus *Reticunassa*, with the description of six new species. *European Journal of Taxonomy* **2017**, 1–43. doi:10.5852/ejt.2017.275

Guindon S, Delsuc F, Dufayard JF, Gascuel O (2009) Estimating maximum likelihood phylogenies with PhyML. *Methods in Molecular Biology* **537**, 113–137. doi:10.1007/978-1-59745-251-9\_6

Hillis DM, Bull JJ (1993) An empirical test of bootstrapping as a method for assessing confidence in phylogenetic analysis. *Systematic Biology* **42**, 182–192. doi:10.1093/sysbio/42.2.182

Kimura M (1980) A simple method for estimating evolutionary rates of base substitutions through comparative studies of nucleotide sequences. *Journal of Molecular Evolution* **16**, 111–120. doi:10.1007/BF01731581

Kittivorachate R, Yangyuen C (2004) Molluscs in the Ubolratana Reservoir, Khon Kaen. *Kasetsart Journal (Natural Science)* **139**, 131–139.

Klingenberg CP (2011) MorphoJ: an integrated software package for geometric morphometrics. *Molecular Ecology Resources* **11**, 353–357. doi:10.1111/j.1755-0998.2010.02924.x

Köhler F, Seddon M, Bogan AE, Van Tu D, Sri-aroon P, Allen D (2010) Chapter 4. The status and distribution of freshwater molluscs of the

- Indo-Burma region. In 'The status and distribution of freshwater biodiversity in Indo-Burma'. (Eds DJ Allen, WRT Darwall, KG Smith) pp. 66–89. (IUCN: Cambridge, UK, and Gland, Switzerland)
- Krailas D, Chotessaengsri S, Dechruksa W, Namchote S, Chuanprasit C, Veeravechskij N, Boonmekam D, Koonchornboon T (2012) Species diversity of aquatic mollusks and their cercarial infections; Khao Yai National Park, Thailand. *The Journal of Tropical Medicine and Parasitology* **35**, 37–47.
- Kumar S, Stecher G, Tamura K (2016) MEGA7: Molecular Evolutionary Genetics Analysis version 7.0 for bigger datasets. *Molecular Biology and Evolution* **33**, 1870–1874. doi:10.1093/molbev/msw054
- Lee CT, Huang CW, Hwang CC, Sutcharit C, Jirapatrasilp P (2022) Arboreal snail genus *Amphidromus* Albers, 1850 of Southeast Asia: shell polymorphism of *Amphidromus cruentatus* (Morelet, 1875) revealed by phylogenetic and morphometric analyses. *PLoS One* **17**, e0272966. doi:10.1371/journal.pone.0272966
- Leigh JW, Bryant D (2015) POPART: full-feature software for haplotype network construction. *Methods in Ecology and Evolution* **6**, 1110–1116. doi:10.1111/2041-210X.12410
- Mekong River Commission (2010) Mekong fisheries and mainstream dams. In 'Mekong River Commission strategic environmental assessment of hydropower on the Mekong mainstream'. (Ed. E Baran) pp. 1–146. (ICEM: Hanoi, Vietnam)
- Neiber MT, Glaubrecht M (2019) *Oligohalinophila*, a new genus for the brackish water assassin snail *Canidia dorri* Wattebled, 1886 from Vietnam (Buccinoidea: Nassariidae: Anentominae). *Journal of Molluscan Studies* **85**, 280–283. doi:10.1093/mollus/eyy065
- Nerurkar S, Shimpi GG, Apte D (2020) First record of *Nassarius fuscus* (Hombron & Jacquinot, 1848) from the west coast of India, with the description of its sister species *Nassarius arewarensis* n. sp. (Buccinoidea: Nassariidae). *Journal of Molluscan Studies* **86**, 240–248. doi:10.1093/MOLLUS/EYAA010
- Olivier L, Schneiderman M (1956) A method for estimating the density of aquatic snail populations. *Experimental Parasitology* **5**, 109–117. doi:10.1016/0014-4894(56)90008-X
- Puillandre N, Brouillet S, Achaz G (2021) ASAP: Assemble Species by Automatic Partitioning. *Molecular Ecology Resources* **21**, 609–620. doi:10.1111/1755-0998.13281
- Rohlf FJ (2015) The tps series of software. *Hystrix, the Italian Journal of Mammalogy* **26**(9), 9–12. doi:10.4404/hystrix-26.1-11264
- Ronquist F, Teslenko M, van der Mark P, Ayres DL, Darling A, Höhna S, Larget B, Liu L, Suchard MA, Huelsenbeck JP (2012) MrBayes 3.2: efficient Bayesian phylogenetic inference and model choice across a large model space. *Systematic Biology* **61**, 539–542. doi:10.1093/sysbio/sys029
- Rozas J, Ferrer-Mata A, Sánchez-DelBarrio JC, Guirao-Rico S, Librado P, Ramos-Onsins SE, Sánchez-Gracia A (2017) DnaSP 6: DNA sequence polymorphism analysis of large datasets. *Molecular Biology and Evolution* **34**, 3299–3302. doi:10.1093/molbev/msx248
- Saitou N, Nei M (1987) The neighbor-joining method: a new method for reconstructing phylogenetic trees. *Molecular Biology and Evolution* **4**, 406–425. doi:10.1093/oxfordjournals.molbev.a040454
- San Mauro D, Agorreta A (2010) Molecular systematics: a synthesis of the common methods and the state of knowledge. *Cellular and Molecular Biology Letters* **15**, 311–341. doi:10.2478/s11658-010-0010-8
- Stanicka A, Maciaszek R, Cichy A, Templin J, Świderek W, Żbikowska E, Labecka AM (2022) Unwanted 'hitchhikers' of ornamental snails: a case report of digeneans transported via the international pet trade. *The European Zoological Journal* **89**, 601–607. doi:10.1080/24750263.2022.2065039
- Strong EE, Galindo LA, Kantor YI (2017) Quid est *Clea helena*? Evidence for a previously unrecognized radiation of assassin snails (Gastropoda: Buccinoidea: Nassariidae). *PeerJ* **5**, e3638. doi:10.7717/peerj.3638
- Suchard MA, Lemey P, Baele G, Ayres DL, Drummond AJ, Rambaut A (2018) Bayesian phylogenetic and phylodynamic data integration using BEAST 1.10. *Virus Evolution* **4**, vey016. doi:10.1093/ve/vey016
- Sullivan J (2005) Maximum-likelihood methods for phylogeny estimation. *Methods in Enzymology* **395**, 757–779. doi:10.1016/S0076-6879(05)95039-8
- Thompson JD, Higgins DG, Gibson TJ (1994) CLUSTAL W: improving the sensitivity of progressive multiple sequence alignment through sequence weighting, position-specific gap penalties and weight matrix choice. *Nucleic Acids Research* **22**, 4673–4680. doi:10.1093/nar/22.22.4673
- von dem Busch G (1847) *Melania*. In 'Abbildungen und beschreibungen neuer oder wenig gekannter conchylien, unter mithilfe mehrer deutscher conchyliologen'. (Ed. RA Philippi) p. 170. (T. Fischer: Cassel) [In German]
- Wiroonpan P, Chontananarth T, Purivirojkul W (2021) Cercarial trematodes in freshwater snails from Bangkok, Thailand: prevalence, morphological and molecular studies, and human parasite perspective. *Parasitology* **148**, 366–383. doi:10.1017/S0031182020002073
- Wiroonpan P, Chontananarth T, Chai JY, Purivirojkul W (2022) High diversity of trematode metacercariae that parasitize freshwater gastropods in Bangkok, Thailand, and their infective situations, morphologies and phylogenetic relationships. *Parasitology* **149**, 913–933. doi:10.1017/S0031182022000312
- Yang J, Zhang S (2011) The radular morphology of Nassariidae (Gastropoda: Caenogastropoda) from China. *Chinese Journal of Oceanology and Limnology* **29**, 1023–1032. doi:10.1007/s00343-011-0079-6
- Yodsiri S, Wongpakam K, Ardhan A, Senakun C, Khumkratok S (2017) Population genetic structure and genetic diversity in twisted-jaw fish, *Belodontichthys truncatus* Kottelat & Ng, 1999 (Siluriformes: Siluridae), from Mekong basin. *International Journal of Zoology* **2017**, 1–7.
- Yutemsuk N, Krailas D, Ananchaenkit C, Phanpeng L, Dechruksa W (2017) Trematode infections of freshwater snails genus *Clea* A. Adams, 1855 in the reservoir of lower northeast Thailand. *Joint International Tropical Medicine Meeting* **6**, 7–16.
- Zhang J, Kapli P, Pavlidis P, Stamatakis A (2013) A general species delimitation method with applications to phylogenetic placements. *Bioinformatics* **29**, 2869–2876. doi:10.1093/bioinformatics/btt499
- Zou S, Li Q, Kong L, Yu H, Zheng X (2011) Comparing the usefulness of distance, monophyly and character-based dna barcoding methods in species identification: a case study of Neogastropoda. *PLoS One* **6**, e26619. doi:10.1371/journal.pone.0026619

**Data availability.** The data supporting this study can be obtained from the corresponding author upon reasonable request.

**Conflicts of interest.** The authors declare that they have no conflicts of interest.

**Declaration of funding.** This research was funded by the Human Resource Development in Science Project (Science Achievement Scholarship of Thailand, SAST) to N. Chomchoei and Chiang Mai University to N. Chomchoei and N. Nantarat. Additional funding came from the Royal Belgian Institute of Natural Sciences (RBINS) to T. Backeljau.

**Acknowledgements.** We are grateful to C. Sutcharit, E. Jeratthitikul, W. Siriwut, R. Srisonchai, S. Chhuoy, K. Pin and P. B. Ngor for assistance in collecting samples. We are also indebted to SMF, Frankfurt for allowing the authors to examine the collections and photographs of type specimens. We are thankful to the Applied Parasitology Research Laboratory for use of laboratory infrastructure. We also thank the anonymous reviewers for critically reviewing the manuscript.

#### **Author affiliations**

<sup>A</sup>PhD Program in Biodiversity and Ethnobiology (International Program), Department of Biology, Faculty of Science, Chiang Mai University, Chiang Mai, 50200, Thailand.

<sup>B</sup>Department of Biology, Faculty of Science, Chiang Mai University, Chiang Mai, 50200, Thailand.

<sup>C</sup>Applied Parasitology Research Laboratory, Department of Biology, Faculty of Science, Chiang Mai University, Chiang Mai, 50200, Thailand.

<sup>D</sup>Royal Belgian Institute of Natural Sciences, Barcoding Facility for Organisms and Tissues of Policy Concern (BopCo), Vautierstraat 29, B-1000 Brussels, Belgium.

<sup>E</sup>Evolutionary Ecology Group, University of Antwerp, Universiteitsplein 1, B-2610 Antwerp, Belgium.

<sup>F</sup>Department of Biology, Faculty of Science, Mahasarakham University, Maha Sarakham, 44150, Thailand.

<sup>G</sup>Institute for Tropical Biology and Conservation, Universiti Malaysia Sabah, Jalan UMS, Kota Kinabalu, 88450, Sabah, Malaysia.

<sup>H</sup>Lee Kong Chian Natural History Museum, National University of Singapore, 2 Conservatory Drive, 117377, Singapore.

<sup>I</sup>Environmental Science Research Center, Faculty of Science, Chiang Mai University, Chiang Mai, 50200, Thailand.